Geophysical Research Letters

RESEARCH LETTER
10.1029/2018GL078621

Key Points:
- Stream discharge increased in numerous streams after earthquakes in Chile
- The magnitude of changes does not increase with increasing peak ground shaking but supports a PGV threshold of >~10 cm/s
- Increased discharge may result from changes in permeability caused by seismic waves

Supporting Information:
- Supporting Information S1
- Table S1

Correspondence to:
C. H. Mohr,
cmohr@uni-potsdam.de

Citation:
Mohr, C. H., Manga, M., & Wald, D. (2018). Stronger peak ground motion, beyond the threshold to initiate a response, does not lead to larger stream discharge responses to earthquakes. *Geophysical Research Letters, 45*, 6523–6531. https://doi.org/10.1029/2018GL078621

Received 3 MAY 2018
Accepted 13 JUN 2018
Accepted article online 21 JUN 2018
Published online 12 JUL 2018

Stronger Peak Ground Motion, Beyond the Threshold to Initiate a Response, Does Not Lead to Larger Stream Discharge Responses to Earthquakes

Christian H. Mohr[1], Michael Manga[2], and David Wald[3]

[1]Institute of Earth and Environmental Sciences, University of Potsdam, Potsdam, Germany, [2]Department of Earth and Planetary Science, University of California, Berkeley, CA, USA, [3]U.S. Geological Survey, Golden, CO, USA

Abstract The impressive number of stream gauges in Chile, combined with a suite of past and recent large earthquakes, makes Chile a unique natural laboratory to study several streams that recorded responses to multiple seismic events. We document changes in discharge in eight streams in Chile following two or more large earthquakes. In all cases, discharge increases. Changes in discharge occur for peak ground velocities greater than about 7–11 cm/s. Above that threshold, the magnitude of both the increase in discharge and the total excess water do not increase with increasing peak ground velocities. While these observations are consistent with previous work in California, they conflict with lab experiments that show that the magnitude of permeability changes increases with increasing amplitude of ground motion. Instead, our study suggests that streamflow responses are binary.

Plain Language Summary Earthquakes deform and shake the surface and the ground below. These changes may affect groundwater flows by increasing the permeability along newly formed cracks and/or clearing clogged pores. As a result, groundwater flow may substantially increase after earthquakes and remain elevated for several months. Here we document streamflow anomalies following multiple high magnitude earthquakes in multiple streams in one of the most earthquake prone regions worldwide, Chile. We take advantage of the dense monitoring network in Chile that recorded streamflow since the 1940s. We show that once a critical ground motion is exceeded, streamflow responses to earthquakes can be expected.

1. Introduction

Following earthquakes, it has long been noted that the amount of water discharged at Earth's surface can increase (e.g., Pliny, the Elder, ca AD 77-79). The magnitude can be substantial, >1 km^3 of excess water in streams (Mohr et al., 2017), and elevated discharge can persist for months (e.g., Liu et al., 2017; Muir-Wood & King, 1993; Rojstaczer et al., 1995). Even dry streams may begin to flow (Wang & Manga, 2015) or streams or ponds may disappear (Curci & Tertulliani, 2015). Further, earthquakes may alter the hydrochemical properties of ground- and stream water, which in turn may affect aquatic biota (Galassi et al., 2014), as well as modify the water available for plants (Mohr et al., 2015).

The mechanisms responsible for increased stream discharge are uncertain. Proposed hypotheses can be grouped into five categories: (1) squeezing water out of aquifers from coseismic contraction (e.g., Muir-Wood & King, 1993), (2) breaking subsurface hydraulic barriers to allow new fluids to reach the surface (e.g., Wang, Manga, et al., 2004), (3) consolidating surface materials (e.g., Montgomery et al., 2003), (4) mobilizing water trapped in the unsaturated zone by ground shaking (Mohr et al., 2015), and (5) increasing permeability (e.g., Briggs, 1991; Rojstaczer & Wolf, 1992; Sato et al., 2000; Tokunaga, 1999; Wang, Wang, & Manga, 2004). In recent years, attempts to test hypotheses have generally favored changes in permeability dominating the response (e.g., Ishitsuka et al., 2017; Mohr et al., 2017; Petitta et al., 2017; Wang & Manga, 2015).

One limitation of most studies in testing hypotheses is that observations are limited to documenting how one or more streams respond to a single earthquake. Documenting responses to multiple earthquakes has proven useful in showing that at least some springs (Manga & Rowland, 2009) and streams (Manga et al., 2003) do not respond to coseismic volumetric strains. Instead, dynamic strains from seismic waves must be responsible for changes in discharge. This is consistent with peak ground velocity (PGV) being the best predictor of whether streams respond to earthquakes (Mohr et al., 2017). However, it remains unclear whether the magnitude of responses scales with the intensity of ground motion, or whether the response

is binary—changes occur if ground motion is large enough, but the magnitude of response is independent of the ground motion beyond some threshold. Distinguishing between these two cases, a scaled or binary response, may help evaluate proposed hypotheses.

Here we take advantage of the large number of earthquakes in Chile and the large number of monitored streams (Mohr et al., 2017) to document the response of multiple streams to multiple earthquakes. We then revisit hypotheses in light of the observations.

2. Data Sets

We searched for streamflow responses to earthquakes in Chile because there is a large number of stream gauges and there are many large $M \geq 8$ earthquakes over the time period with gauging data. In total, there are records from 716 streamflow gauging stations and complementary rainfall records at 802 gauges (http://dgasatel.mop.cl/). Not all gauges have data that overlap with all earthquakes. Here we examine responses to six $M \geq 8$ earthquakes that occurred since the M9.5 1960 earthquake (see Table S1 in the supporting information). Both the streamflow and rainfall gauges are clustered in central and southern-central Chile. Given that the rain gauges are not equally distributed across Chile and their number has been increasing over time (since 1940), we considered the five closest rainfall gauges to the respective catchment, which in turn yielded maximum distances of $\leq$33 km between both. We chose five rainfall gauges to ensure they are close enough to be relevant and capture precipitation events that might affect streamflow.

3. Methods

First, we visually check the hydrographs for streamflow responses to the earthquakes. To this end, we preselect streamflow data available at the time of the earthquakes. Second, given coverage of rain gauges, we check for potential rainfall effects on streamflow. Third, in the case of data gaps in the rainfall time series, we perform recession analyses to check whether the streamflow changes can be attributed to quick flow or base flow (Blume et al., 2007; Reusser, 2014). Recession analysis measures the rate of decrease of discharge during periods without recharge, and the rate scales with permeability (e.g., Blume et al., 2007). We also require that earthquake responses persist and can be recognizable for several days, here for $>$4 days before the streamflow responses are obscured by rainfall (Figure S1.2. in the supporting information).

We characterize ground motion by the PGV because this measure of ground motion is best able to classify whether or not streams respond to earthquakes (e.g., Mohr et al., 2017). We extract PGV from U.S. Geological Survey ShakeMaps (Worden & Wald, 2016), with versions and details summarized in Table S3. PGVs provided by ShakeMap combine the maximum value observed on the two horizontal components of motion. PGV is estimated by converted macroseismic intensity observations using ground motion to intensity conversion equations, with both augmented by ground motion prediction where there are few data (Worden & Wald, 2016). We do not compare responses with static volumetric strains because a previous analysis of the response to the 2010 M8.8 Maule earthquake and studies elsewhere found no general correlation between the sign of the volumetric strain and the sign of the discharge change (e.g., Mohr et al., 2017).

In order to extract the total amount of excess water, we fit a groundwater flow model to the observations. The model neglects quick flow since rainfall was not registered nor does recession analysis point to quick flow (in the case of incomplete rainfall time series). We follow previous studies (e.g., Manga et al., 2016; Mohr et al., 2017; Wang, Manga, et al., 2004) by using a one-dimensional groundwater flow model in which excess water is made available, either by changing vertical permeability (Wang, Wang, & Manga, 2004) or releasing water from storage (Manga et al., 2003). Both result in a coseismically elevated hydraulic head. We assume that the change in hydraulic head h at position x is governed by the one-dimensional groundwater flow equation

$$\frac{\partial h}{\partial t} = D\frac{\partial^2 h}{\partial x^2} \tag{1}$$

with discharge Q given by

$$Q = -\frac{\partial h}{\partial x} K A_{t,} \tag{2}$$

where t is time, D is the hydraulic diffusivity, and A_t is the cross-section area through which water discharges into the stream. The aquifer extends from $x = 0$ at the catchment divide, where $\partial h/\partial x = 0$, to $x = L$ at the

stream with $h(L, t) = 0$. At the time of the earthquake h increases over the region $0 < x < L'$ such that the total excess water is Q_{excess}. The solution for Q as a function of time t since the earthquake is (Mohr et al., 2017)

$$Q(t) = Q_0 e^{-\pi Dt/4L^2} + \frac{2DQ_{excess}}{LL'} \sum_{r=1}^{\infty} (-1)^{r-1} \sin \frac{(2r-1)\pi L'}{2L} e^{-\frac{(2r-1)\pi^2 D}{4L^2} t} \quad (3)$$

where the first term accounts for the base flow recession that would have occurred in the absence of the earthquake and r is the summation index. The model is fit to the daily postseismic discharge measurements predating any precipitation events by minimizing the least squares residual using the Gauss-Newton algorithm implemented in R (R Core Team, 2017). Our modeling approach comprises two steps. First, we model all streamflow responses individually; that is, we fit the model considering the three parameters L'/L, D/L^2 (d^{-1}), and Q_{excess} (mm). In the second step, we average the catchment-specific permeability values (D/L^2) obtained for each individual hydrograph. Hence, we reduce the modeling parameters here to two, that is, L/L' and Q_{excess}. Table S2 summarizes the parameterization. We estimate Q_{excess} and relative streamflow increase (%) as a function of PGV using bootstrapped linear modeling to search for scalings between ground motion and the magnitude of streamflow responses.

We also explore threshold value (s) of PGV needed to trigger changes in streamflow. We compare a total of $n = 110$ responding and $n = 116$ nonresponding streams with the catchment specific PGVs. In order to separate responding from nonresponding streams, we test several statistical/machine learning algorithms: decision tree classifier (CART; R Core Team, 2017), logistic regression modeling (R Core Team, 2017), and Random Forest (Breiman, 2001; Liaw & Wiener, 2002). All details are given in Text S1 in the supporting information.

4. Results

Figure 1 shows the eight catchments for which we could identify two or more responses to earthquakes. The earthquakes that triggered the multiple streamflow responses are the *M*9.5 1960 Valdivia, *M*8.0 1985 Valparaiso, and/or the *M*8.8 2010 Maule earthquake. In all cases, when there was a response, discharge increased. All other earthquakes (Tables S1 and S3) also triggered streamflow anomalies. These responses, however, did not contribute to the subset of responses that occurred in at least two streams.

Figure 1 also shows the measured and modeled hydrographs for four representative example hydrographs. All other modeled streamflow responses are shown in Figures S1.1–S1.4. In general, the idealized model (equation (3)) fits the observations well. The corresponding R^2 ranged between 0.58 and 0.97 for the Alicahue @ Colliguay during the 2010 earthquake and the Chillan @ Esperanza during the 1960 earthquake, respectively. We identified different permeability values for the same catchment during different earthquakes (see Table S2). This is the case for responses of the Alicahue River for the 1985 and 2010 responses or the Uble River when compared to the averaged permeability values. At the same time, though, the averaged permeability value for the Claro River fits data for all three earthquakes.

Figure 2 compares the magnitude of responses, both the peak postseismic discharge compared with preseismic discharge $\Delta Q/Q$ and the total excess water Q_{excess}, as a function of the PGV. We do not see a continuously increasing response with increasing PGV, that is, a scaling between the magnitude of ground motion and the magnitude of streamflow increase. Instead, there appears to be a threshold to initiate a response. Figure 3 shows the density curves for both responses and nonresponses as a function of PGV. Our data identify threshold values for PGV separating responding ($n = 110$) from nonresponding ($n = 116$) streams. These data points include all streams that responded to earthquakes, not only those that responded to multiple events. Using logistic regression, we obtain a threshold of ~11.2 cm/s for $p = 0.5$ (see Text S1), a value that is slightly higher than for a simple classification tree approach (~6.7 cm/s). Both models, however, have limited performance. The misclassification rates are ~34–39% (Figure 3), and there are responses to PGV lower than these statistically identified thresholds (Figure 2).

5. Discussion

Documenting responses to multiple earthquakes allows us to address some of the open questions highlighted in the introduction.

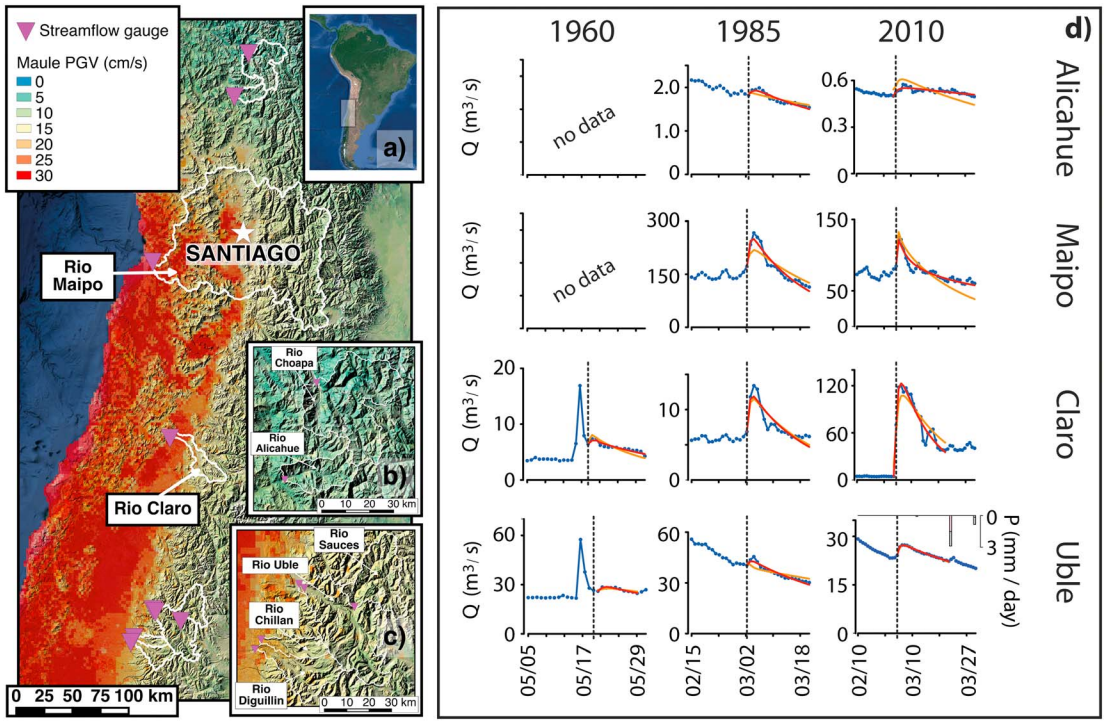

Figure 1. Geographical setting of catchments (white polygons) and sample hydrographs. (a) Ground motion expressed as peak ground velocity for the *M*8.8 Maule earthquake, overlain on Shuttle Radar Topography Mission topography; bathymetry from Google Earth. (b and c) More detailed view of the clustered catchments that responded to multiple earthquakes. Sample hydrographs (d) showing postseismic increases in stream discharge. The blue dotted line is measured streamflow discharge (m^3/s); histogram shows precipitation (mm/d) if data are available and rainfall occurred. The red and orange curves are fits from modeled streamflow discharge (m^3/s; equation (3)). The red curve (model 1) depicts the response to an individual model fit, the orange curve (model 2), instead, considers the mean permeability values of streams responding to multiple earthquakes. The black dashed line indicates the time of the earthquakes.

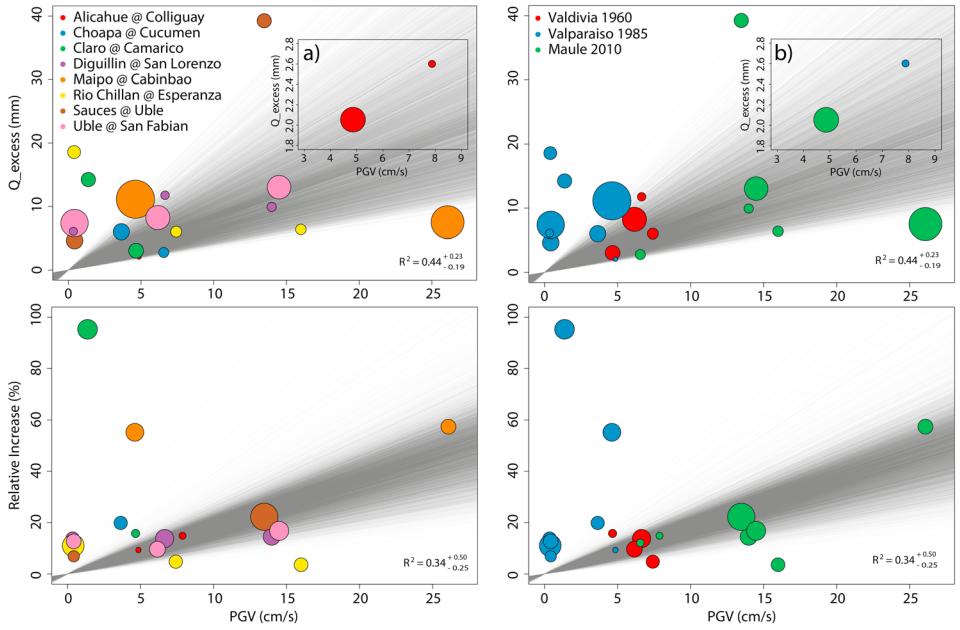

Figure 2. Magnitude of the streamflow responses to the Valdivia (n = 4), Valparaiso (n = 8), and Maule (n = 8) earthquakes expressed as a function of peak ground velocity. Bubble size scales with coseismic discharge Q_0. (top row) Modeled excess water (mm). (bottom row) Maximum postseismic discharge relative to coseismic discharge (%). (left column) Responses by stream and (right) column by earthquake. (a and b) Data that are hidden by other responses in the main plots. R^2 is calculated as the median of 10^5 bootstrapped linear regressions (gray lines), uncertainty is given as 95% confidence intervals.

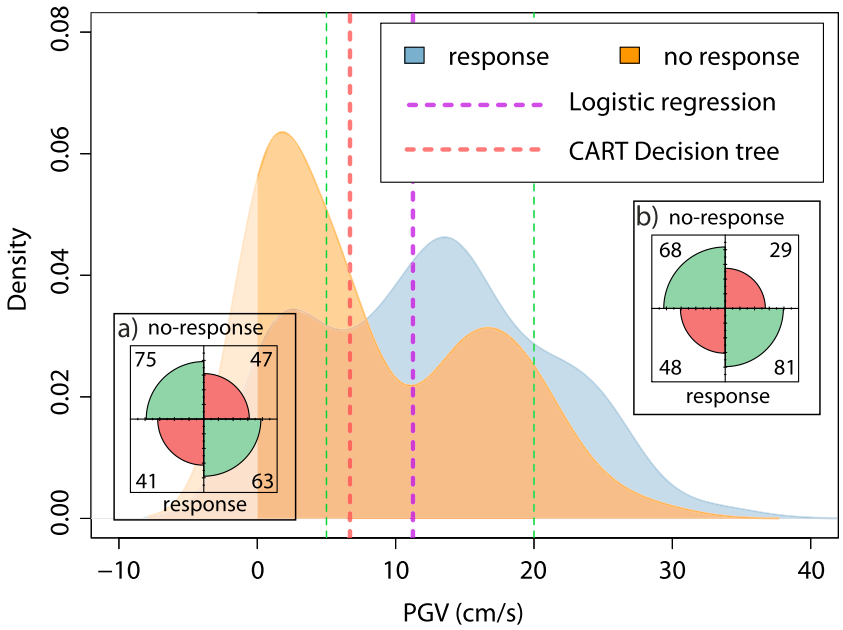

Figure 3. Density curves for all recorded responses (n = 110) and nonresponses (n = 116) to the studied catchments as a function of peak ground velocity (PGV). The green dashed lines enclose the PGV threshold identified in California (Manga et al., 2003). Note: Our PGV data do not cover entire Chile for the studied earthquakes because we cannot expect streamflow responses where PGV = 0. The insets show the confusion matrices for the (a) logistic regression classification and the (b) decision trees classification. Correct classification is indicated by green, misclassification by red. (top row) No-response and (bottom row) response classification. Note: The shaded area (PGV $<$ 0) is intended to highlight that PGV $<$ 0 is impossible and is an artifact of the density curves calculated by Gaussian kernel densities; $n = 10^5$ bootstrapped Kruska-Wallis-tests yield $p = 0.484 \pm 0.186$ between responses and no responses.

5.1. Gradual or Binary Streamflow Responses to Earthquakes

Mohr et al. (2017) identified 85 streams that responded to the 2010 M8.8 Maule earthquake, of which 78 increased their discharge. Of these, only eight responded to at least one other earthquake. This, however, is not surprising, because the areas that ruptured during each of the large $M \geq 8$ earthquakes largely do not overlap (Melnick et al., 2009; Ruiz et al., 2017; Vigny et al., 2011) and hence the regions with the strongest ground shaking also have little overlap.

In contrast to lab experiments (e.g., Candela et al., 2014), our results show that the magnitude of responses does not scale with the amplitude of ground motion. Instead, we identify a threshold PGV of about 10 cm/s to initiate changes in streamflow (Figure 3). Our findings thus favor a binary response, that is, that streamflow changes occur if ground motion is large enough, but the magnitude of response is independent of the ground motion beyond the threshold. Comparable threshold values (5–20 cm/s PGV) are reported from California (Manga et al., 2003). Similarly, Cox et al. (2015) report a threshold for PGA of 0.5% g for springs in New Zealand to respond to earthquakes. Here we do not explicitly explore potential environmental controls on the multiple streamflow responses. A previous study was unable to identify hydrogeological, tectonic, or land cover controls (Mohr et al., 2017). The strongest predictors for whether a stream responded to the Maule earthquake were PGV and PGA, with the former slightly outperforming the latter (Mohr et al., 2017).

5.2. Mechanisms for Causing Discharge to Increase

One of the objectives of our analysis is to use responses to variable forcing to test hypotheses. We thus compare each of the five classes of hypothesis mentioned in the introduction with the observations.

5.2.1. Static Strain

Muir-Wood and King (1993) showed that magnitude and distribution of streamflow responses to the Hebgen Lake and Borah Peak earthquakes roughly mimic the pattern of volumetric strain computed from deformation models. Similarly, Jonsson et al. (2003) documented a pattern of water-level changes that

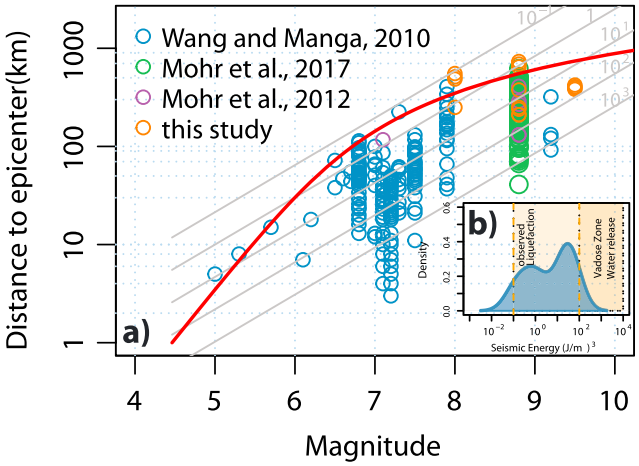

Figure 4. Earthquake magnitude-distance relationship. (a) Seismically triggered streamflow changes (circles) as a function of earthquake magnitude and distance from epicenter. The blue circles are data from Wang and Manga (2010a); the violet circles are data from the Maule earthquake, and the *M*7.1 2011 Araucania aftershock in Chilean headwater catchments (Mohr et al., 2012); the green circles are data from Maule earthquake (Mohr et al., 2017). The orange circles are data from this study. The red solid line is an empirical bound for liquefaction (Papadopoulos & Lefkopoulos, 1993). The gray lines are seismic energy density (J/m^3; Wang & Manga, 2010b). (b) Seismic energy density estimated for the studied catchments and domains for liquefaction (Wang & Manga, 2010b) and release of soil water in nearly saturated sandy soils (Mohr et al., 2015).

follows the distribution of volumetric strain. Assuming that static strain is responsible for the changes, the magnitude of the response should scale with the magnitude of static strain. The lack of correlation of the sign of the response with the sign of the strain for the Maule earthquake (Mohr et al., 2017), however, does not favor this mechanism as a dominant source for the excess water. This is consistent with findings by previous studies that evaluated hydrological responses to multiple earthquakes (e.g., Manga et al., 2003; Manga & Rowland, 2009; Shi et al., 2014, 2015). Hence, we favor dynamic strain as the trigger for responses.

5.2.2. New Fluid Sources

If subsurface barriers are breached, we might expect a threshold in the ground motion. Our findings are thus consistent with this conceptual model. Midcrustal fault displacement processes that expel fluids may increase water temperature and change hydrochemistry (Wang & Manga, 2010a), though the addition of deeper or new fluids need not change hydrogeochemistry. Owing to the lack of hydrogeochemical and water temperature data, we cannot reject this hypothesis. However, where we have data from previous studies (Mohr et al., 2012), we do not find supporting evidence.

5.2.3. Compaction and Liquefaction

Based on an empirical magnitude-distance relationship (Papadopoulos & Lefkopoulos, 1993) and seismic energy thresholds (Wang, 2007), liquefaction in many of the catchments may be possible (Figure 4). Our observed responses for the Maule and particularly the Valparaiso earthquakes document some of the most sensitive streamflow responses to earthquakes observed worldwide. In our analysis, we consider only peak ground motion, and not shaking duration. The number of loading cycles is a significant factor for triggering liquefaction due to pore pressure buildup (Holzer et al., 1989) and may be a factor in streamflow response (Montgomery & Manga, 2003). However, duration in regional liquefaction studies is typically accommodated only approximately with a magnitude scaling factor (e.g., Zhu et al., 2017) and is not routinely quantified in postearthquake products such as ShakeMap.

Stronger shaking should cause more widespread liquefaction and consolidation and hence larger responses. We do not see, however, increasing responses with increasing ground motion (Figure 2). Moreover, surface manifestations of liquefaction are not documented in all the settings with increased discharge (Mohr et al., 2017), though widespread liquefaction following the Maule earthquake was reported for saturated floodplains up to an epicentral distance of approximately 1,000 km (Verdugo & González, 2015). Liquefaction was also observed during the Valparaiso earthquake (Algermissen, 1985) and following the Valdivia earthquakes, but the latter is less well documented. Furthermore, responses occurred within headwater catchments of the Andes and the Coastal Mountains where liquefaction-prone sediments or soils, such as sandy saturated soils, are not dominant (Casanova et al., 2013). In addition, two of the three studied earthquakes (Valparaiso and Maule earthquakes) occurred during the dry season. Taken together, we cannot favor undrained consolidation or liquefaction as dominant processes.

5.2.4. Shaking Water out of Soils

The hypothesis that water is mobilized from the unsaturated zone assumes that ground deformation transfers energy to overcome the matric potential retaining water in soils. One key requirement is a connectivity between the unsaturated and saturated zone (Mohr et al., 2015). Assuming comparable soil texture, we would expect the magnitude of responses to depend both on the amplitude of strains and the amount of water that is available by shaking. Judging from the literature (Casanova et al., 2013), however, we can only speculate about the soil texture in the catchments. We neither know the soil water contents prior to and after the earthquakes except for parts of the Coastal Mountain Range (Ghislaine et al., 2012; Mohr et al., 2012) during the Maule earthquake.

Because the Valparaiso earthquake occurred later in the dry season than the Maule earthquake, for similar PGV, we should expect less excess water for the same catchments. This is not what we observe (Figure 2).

The earthquakes occurred during different seasons of the year. Hence, comparing saturated soils during austral winter (Valdivia earthquake) with dry soils during austral summer (Maule and Valparaiso earthquakes) is problematic. Nevertheless, we can compare the distinct responses for each earthquake separately. When normalized for the climatic conditions, we would expect either an excess water-PGV or a relative increase-PGV scaling. This is not what we observe (Figure 2).

5.2.5. Increased Permeability

By monitoring the responses of water level in a well to solid Earth tides, Elkhoury et al. (2006) showed that regional earthquakes increase permeability and that the magnitude of permeability changes increases with increasing PGV. Lab experiments similarly showed that increasing the amplitude of oscillatory flows increases the permeability change (e.g., Candela et al., 2014). We do not see such relationships (Figure 2). Though uncommon, decreased permeability after earthquakes has also been reported (Shi et al., 2018).

Recession constants can be used to characterize the hydraulic conductivity along dominant flow paths, typically parallel to bedding and within the most permeable formations. Recession analysis cannot, however, identify where changes occur nor can it characterize changes in an anisotropic system. Here postseismic changes in lateral permeability are not substantial (see Figure S2). We thus argue that enhanced lateral permeability is not the reason for the observed streamflow responses.

Instead, our results are consistent with the enhanced vertical permeability, for example, by breaching impervious geological layers via subvertical cracks (Wang et al., 2016) or clearing clogged pore throats (Candela et al., 2014). This model elevates the hydraulic head after water has been released from higher areas (Wang, Wang, & Manga, 2004) enhancing recharge in elevated areas and discharge at hillslope toes, consistent with topographical shape of a catchment that is a response predictor (Mohr et al., 2017).

Postseismic recovery of permeability may be geologically fast, for example, months (Elkhoury et al., 2006) to years (Xue et al., 2013). Assuming complete recovery during interseismic periods, we might expect constant catchment-characteristic permeability, and thus, differences between the modeled responses using either catchment-averaged permeability or earthquake-specific model parameterization should be small. This is the case for the Claro river (Figure 1) and also Chillan river (Figure S1.4). In contrast, other catchments, for example, the Alicahue or Uble rivers, exhibit large differences among the fitted model parameters. Consequently, our study suggests complete recovery of permeability during 25 years for some but not all studied catchments.

6. Summary and Conclusions

Despite the large number of large earthquakes and gauged streams in Chile, we could only find eight streams with clear responses to two or more earthquakes. This highlights the challenge in documenting responses of a given stream to multiple earthquakes. For the streams that did respond multiple times, we observe that the magnitude of responses does not scale with increasing amplitude of ground shaking. In contrast, our results suggest a binary response with a threshold value of PGV of approximately 10 cm/s, above which the magnitude of the response is independent of the magnitude of ground motion. The conflict with lab experiments that suggest a scaling between permeability change and ground motion highlights the limited transferability of small-scale experiments to catchment-scale studies. Finally, our study has implications for hydrological modeling. We show that the assumed stationarity of catchment-specific hydraulic parameters, such as permeability, may not be a good assumption for studies that cover time periods longer than interseismic periods in areas frequently struck by earthquakes.

Acknowledgments

M.M. is supported by NSF grant EAR1344424. We thank DGA for collecting data over many decades and then freely sharing them. We ran all computations using the software R. All data are available in the supporting tables or accessible on the Internet as mentioned in the main text and supporting material. We appreciate the constructive comments of two anonymous reviewers and Francis Rengers and Valery Ivanov for handling our manuscript.

References

Algermissen, S. T. (1985). Preliminary report of investigations of the central Chile earthquake of March 3, 1985. U.S. Geological Survey Report, 85–542.

Blume, T., Zehe, E., & Bronstert, A. (2007). Rainfall-runoff response, event-based runoff coefficients and hydrograph separation. *Hydrological Sciences Journal*, *52*(5), 843–862. https://doi.org/10.1623/hysj.52.5.843

Breiman, L. (2001). Random Forests. *Machine Learning*, *45*(1), 5–32. https://doi.org/10.1023/A:1010933404324

Briggs, R. O. (1991). Effects of Loma-Prieta earthquake on surface waters in Waddell Valley. *Water Resources Bulletin*, *27*(6), 991–999. https://doi.org/10.1111/j.1752-1688.1991.tb03148.x

Candela, T., Brodsky, E. E., Marone, C., & Elsworth, D. (2014). Laboratory evidence for particle mobilization as a mechanism for permeability enhancement via dynamic stressing. *Earth and Planetary Science Letters*, *392*, 279–291. https://doi.org/10.1016/j.epsl.2014.02.025

Casanova, M., Salazar, O., Seguel, O., & Luzio, W. (2013). *The soils of Chile*. Dordrecht, Netherlands: Springer. https://doi.org/10.1007/978-94-007-5949-7

Cox, S. C., Menzies, C. D., Sutherland, R., Denys, P. H., Chamberlain, C., & Teagle, D. A. H. (2015). Changes in hot spring temperature and hydrogeology of the Alpine Fault hanging wall, New Zealand, induced by distal South Island earthquakes. *Geofluids*, *15*(1–2), 216–239. https://doi.org/10.1111/gfl.12093

Curci, L., & Tertulliani, A. (2015). The hydrological signature of a seismogenic source: Coseismic hydrological changes in response to the 1915 Fucino (Central Italy) earthquake. *Geophysical Journal International*, *200*(3), 1374–1388. https://doi.org/10.1093/gji/ggu448

De'ath, G., & Fabricius, K. E. (2000). Classification and regression trees: A powerful yet simple technique for ecological data analysis. *Ecology*, *81*, 3178–3192. https://doi.org/10.1890/0012-9658(2000)081[3178:CARTAP]2.0.CO;2

Elkhoury, J. E., Brodsky, E. E., & Agnew, D. C. (2006). Seismic waves increase permeability. *Nature*, *441*(7097), 1135–1138. https://doi.org/10.1038/nature04798

Galassi, D. M. P., Lombardo, P., Fiasca, B., Di Cioccio, A., Di Lorenzo, T., Petitta, M., et al. (2014). Earthquakes trigger the loss of groundwater biodiversity. *Scientific Reports*, *4*, 6273. https://doi.org/10.1038/srep06273

Ghislaine, R., Güntner, A., Creutzfeldt, B., Wziontek, H., Klügel, T., & Tume, et al. (2012). Relación de la variación del almacenamiento de agua local y el gravímetro superconductor en el Observatorio Geodésico TIGO, Concepción, Chile. *Obras y proyectos*, *12*(12), 71–78. https://doi.org/10.4067/S0718-28132012000200006

Hastie, T., Tibshirani, R., & Freidman, J. (2009). *The elements of statistical learning—Data mining, inference, and prediction*. New York: Springer.

Holzer, T. L., Hanks, T. C., & Youd, T. L. (1989). Dynamics of liquefaction during the 1987 Superstition Hills, California, earthquake. *Science*, *244*(4900), 56–59. https://doi.org/10.1126/science.244.4900.56

Ishitsuka, K., Matsuoka, T., Nishimura, T., Tsuji, T., & ElGharbawi, T. (2017). Ground uplift related to permeability enhancement following the 2011 Tohoku earthquake in the Kanto Plain, Japan. *Earth, Planets and Space*, *69*(1), 81. https://doi.org/10.1186/s40623-017-0666-7

Jonsson, S., Segall, P., Pedersen, R., & Bjornsson, G. (2003). Post-earthquake ground movements correlated to pore-pressure transients. *Nature*, *424*(6945), 179–183. https://doi.org/10.1038/nature01776

Liaw, A., & Wiener, M. (2002). Classification and regression by Random Forest. *R News*, *2*(3), 18–22.

Liu, C. Y., Chia, Y., Chuang, P. Y., Wang, C.-Y., Ge, S., & Teng, M. H. (2017). Streamflow changes in the vicinity of seismogenic fault after the 1999 Chi-Chi earthquake. *Pure and Applied Geophysics*. https://doi.org/10.1007/s00024-017-1670-3

Manga, M., Brodsky, E. E., & Boone, M. (2003). Response of streamflow to multiple earthquakes. *Geophysical Research Letters*, *30*(5), 1214. https://doi.org/10.1029/2002GL016618

Manga, M., & Rowland, J. C. (2009). Response of Alum Rock springs to the October 30, 2007 Alum Rock earthquake and implications for the origin of increased discharge after earthquakes. *Geofluids*, *9*(3), 237–250. https://doi.org/10.1111/j.1468-8123.2009.00250.x

Manga, M., Wang, C. Y., & Shirzaei, M. (2016). Increased stream discharge after the 3 September 2016 M-w 5.8 Pawnee, Oklahoma earthquake. *Geophysical Research Letters*, *43*, 11,588–11,594. https://doi.org/10.1002/2016GL071268

Melnick, D., Bookhagen, B., Strecker, M. R., & Echtler, H. P. (2009). Segmentation of megathrust rupture zones from fore-arc deformation patterns over hundreds to millions of years, Arauco peninsula, Chile. *Journal of Geophysical Research*, *114*, B01407. https://doi.org/10.1029/2008JB005788

Mohr, C. H., Manga, M., Wang, C.-Y., Kirchner, J. W., & Bronstert, A. (2015). Shaking water out of soil. *Geology*, *43*(3), 207–210. https://doi.org/10.1130/G36261.1

Mohr, C. H., Manga, M., Wang, C.-Y., & Korup, O. (2017). Regional changes in streamflow after a megathrust earthquake. *Earth and Planetary Science Letters*, *458*, 418–428. https://doi.org/10.1016/j.epsl.2016.11.013

Mohr, C. H., Montgomery, D. R., Huber, A., Bronstert, A., & Iroumé, A. (2012). Streamflow response in small upland catchments in the Chilean coastal range to the M-W 8.8 Maule earthquake on 27 February 2010. *Journal of Geophysical Research*, *117*, F02032. https://doi.org/10.1029/2011JF002138

Montgomery, D. R., Greenberg, H. M., & Smith, D. T. (2003). Streamflow response to the Nisqually earthquake. *Earth and Planetary Science Letters*, *209*(1–2), 19–28. https://doi.org/10.1016/S0012-821X(03)00074-8

Montgomery, D. R., & Manga, M. (2003). Streamflow and water well responses to earthquakes. *Science*, *300*(5628), 2047–2049. https://doi.org/10.1126/science.1082980

Muir-Wood, R., & King, G. C. P. (1993). Hydrological signatures of earthquake strain. *Journal of Geophysical Research*, *98*, 22,035–22,068. https://doi.org/10.1029/93JB02219

Nathan, R. J., & McMahon, T. A. (1990). Evaluation of automated techniques for base flow and recession analyses. *Water Resoures Research*, *26*, 1465–1473. https://doi.org/10.1029/WR026i007p01465

Papadopoulos, G. A., & Lefkopoulos, G. (1993). Magnitude-distance relations for liquefaction in soil from earthquakes. *Bulletin of the Seismological Society of America*, *83*(3), 925–938.

Petitta, M., Mastrorillo, L., Preziosi, E., Banzato, F., Barberio, M. D., Billi, A., et al. (2017). Water-table and discharge changes associated with the 2016–2017 seismic sequence in central Italy: Hydrogeological data and a conceptual model for fractured carbonate aquifers. *Hydrogeology Journal*, *26*(4), 1009–1026. https://doi.org/10.1007/s10040-017-1717-7

Pliny, the Elder, ca AD 77–79. The Natural History.

R Core Team (2017). R: A language and environment for statistical computing. R Foundation for Statistical Computing. Vienna.

Reusser, D. (2014). Tiger: TIme series of Grouped ERrors.

Rojstaczer, S., & Wolf, S. (1992). Permeability changes associated with large earthquakes—An example from Loma-Prieta, California. *Geology*, *20*(3), 211–214. https://doi.org/10.1130/0091-7613(1992)020<0211:PCAWLE>2.3.CO;2

Rojstaczer, S., Wolf, S., & Michel, R. (1995). Permeability enhancement in the shallow crust as a cause of earthquake-induced hydrological changes. *Nature*, *373*(6511), 237–239. https://doi.org/10.1038/373237a0

Ruiz, S., Moreno, M., Melnick, D., del Campo, F., Poli, P., Baez, J. C., et al. (2017). Reawakening of large earthquakes in south central Chile: The 2016 M-w 7.6 Chiloe event. *Geophysical Research Letters*, *44*, 6633–6640. https://doi.org/10.1002/2017GL074133

Sato, T., Sakai, R., Furuya, K., & Kodama, T. (2000). Coseismic spring flow changes associated with the 1995 Kobe earthquake. *Geophysical Research Letters*, *27*, 1219–1222. https://doi.org/10.1029/1999GL011187

Shi, Z. M., Wang, G. C., Wang, C. Y., Manga, M., & Liu, C. L. (2014). Comparison of hydrological responses to the Wenchuan and Lushan earthquakes. *Earth and Planetary Science Letters*, *391*, 193–200. https://doi.org/10.1016/j.epsl.2014.01.048

Shi, Z., Wang, G., Manga, M., & Wang, C. Y. (2015). Mechanism of co-seismic water level change following four great earthquakes-insights from co-seismic responses throughout the Chinese mainland. *Earth and Planetary Science Letters*, *430*, 66–74.

Shi, Z. M., Zhang, S. C., Yan, R., & Wang, G. C. (2018). Fault zone permeability decrease following large earthquakes in a hydrothermal system. *Geophysical Research Letters*, *45*, 1387–1394. https://doi.org/10.1002/2017gl075821

Strobl, C., Boulesteix, A. L., Kneib, T., Augustin, T., & Zeileis, A. (2008). Conditional variable importance for Random Forests. *BMC Bioinformatics*, *9*(1), 307. https://doi.org/10.1186/1471-2105-9-307

Tokunaga, T. (1999). Modeling of earthquake-induced hydrological changes and possible permeability enhancement due to the 17 January 1995 Kobe earthquake, Japan. *Journal of Hydrology*, *223*(3–4), 221–229. https://doi.org/10.1016/S0022-1694(99)00124-9

Verdugo, R., & González, J. (2015). Liquefaction-induced ground damages during the 2010 Chile earthquake. *Soil Dynamics and Earthquake Engineering*, *79*, 280–295. https://doi.org/10.1016/j.soildyn.2015.04.016

Vigny, C., Socquet, A., Peyrat, S., Ruegg, J.-C., Métois, M., Madariaga, R., et al. (2011). The 2010 M8.8 Maule megathrust earthquake of Central Chile, monitored by GPS. *Science*, *332*(6036), 1417–1421. https://doi.org/10.1126/science.1204132

Wang, C. Y. (2007). Liquefaction beyond the near field. *Seismological Research Letters*, *78*(5), 512–517. https://doi.org/10.1785/gssrl.78.5.512

Wang, C.-Y., Liao, X., Wang, L.-P., Wang, C.-H., & Manga, M. (2016). Large earthquakes create vertical permeability by breaching aquitards. *Water Resources Research*, *52*, 5923–5937. https://doi.org/10.1002/2016WR018893

Wang, C. Y., & Manga, M. (2010a). *Earthquakes and water, lecture notes in Earth sciences*. Berlin, Heidelberg: Springer.

Wang, C. Y., & Manga, M. (2010b). Hydrologic responses to earthquakes and a general metric. *Geofluids*, *10*, 206–216. https://doi.org/10.1002/9781444394900.ch14

Wang, C.-Y., & Manga, M. (2015). New streams and springs after the 2014 Mw6.0 South Napa earthquake. *Nature Communications*, *6*, 7597. https://doi.org/10.1038/ncomms8597

Wang, C. Y., Manga, M., Dreger, D., & Wong, A. (2004). Streamflow increase due to rupturing of hydrothermal reservoirs: Evidence from the 2003 San Simeon, California, earthquake. *Geophysical Research Letters*, *31*, L10502. https://doi.org/10.1029/2004GL020124

Wang, C. Y., Wang, C. H., & Manga, M. (2004). Coseismic release of water from mountains: Evidence from the 1999 (M-W=7.5) Chi-Chi, Taiwan, earthquake. *Geology*, *32*(9), 769–772. https://doi.org/10.1130/G20753.1

Worden, C. B., & Wald, D. J. (2016). ShakeMap manual online: Technical manual, user's guide, and software guide. U.S. Geological Survey. https://doi.org/10.5066/F7D21VPQ

Xue, L., Li, H.-B., Brodsky, E. E., Xu, Z.-Q., Kano, Y., Wang, H., et al. (2013). Continuous permeability measurements record healing inside the Wenchuan earthquake fault zone. *Science*, *340*(6140), 1555–1559. https://doi.org/10.1126/science.1237237

Zhu, J., Baise, L. G., & Thompson, E. M. (2017). An updated geospatial liquefaction model for global application. *Bulletin of the Seismological Society of America*, *107*(3), 1365–1385. https://doi.org/10.1785/0120160198